Structure and Optical Properties of CuInSe$_2$ and Cu$_{0.9}$In$_{0.9}$Zn$_{0.2}$Se$_2$ Thin Films Deposited by One-step Radio-frequency Magnetron Sputtering

WANG Wei-Jun, HE Jun, ZHANG Ke-Zhi, TAO Jia-Hua, SUN Lin, CHEN Ye, YANG Ping-Xiong, CHU Jun-Hao

(Key Laboratory of Polar Materials and Devices, Ministry of Education, Department of Electronic Engineering, East China Normal University, Shanghai 200241, China)

Abstract: CuInSe$_2$ (CIS) and Cu$_{0.9}$In$_{0.9}$Zn$_{0.2}$Se$_2$ (CIZS) thin films were deposited by Radio-Frequency (RF) magnetron sputtering process. X-ray diffraction (XRD) results indicate CIZS film deposited at 300℃ (CIZS-300) is (220) preferred orientation which is different from (112) preferred orientation of other films. Cu-poor and appropriate temperature are major factors for (220) preferred orientation of grains. The Raman spectra show a strong peak around 171 cm^{-1} and a weak peak around 206 cm^{-1}, which corresponding to A$_1$ and B$_2$ modes. Substitution of Zn for Cu leads to a broadening and blue-shift of A$_1$ Raman mode. The band gap E_{opt} of CIZS film increases due to a reduced Se p-Cu d interband repulsion with Zn doping. Scanning electron microscope (SEM) measurement demonstrates that the surface morphology of CIZS is more compact and smoother than that of CIS thin films.

Key words: magnetron sputtering; CIZS thin film; Zn doping

CuInSe$_2$ (CIS) has drawn great attention for its high-absorption coefficient about 10^4–10^5 cm^{-1} as one of the potential materials for absorber layer in solar cell applications, which belongs to the ternary compounds of A^{I}B^{III}C^{IV} type. However, the metal In is rare and expensive which is difficult for the quantity production. Hence, seeking for other more economic elements with good optical performance is extremely urgent. Recently, CuInZnSe$_2$ (CIZS) has become one of the most promising candidates since the first successful fabrication of CuInZnSe$_2$ solar cell[1-2].

CIZS belongs to I-II-III-VI$_2$ group, and has the same chalcopyrite structure with CIS. Furthermore, the band gap (E_{opt}) of ZnSe is 2.67 eV, so CIZS thin films may have chance to obtain the optimal band gap. Several reports have pointed out that the Zn^{2+} would replace randomly Cu$^+$ or In^{3+} in 50% possibilities, respectively[3]. Moreover, the heterovalent exchange of Cu$^+$ and In^{3+} by 2Zn^{2+} would reduce the deformation around the anions because of the similar radii of Cu$^+$(r=0.635) and Zn^{2+}(r=0.640) against In^{3+}(r=0.765) with the 4 coordinate-number[4]. Thus, CIZS is expected to have a great promising application in the absorber layer of thin film solar cells. Some research have revealed that though Zn doping can increase the band gap, high Zn concentration may lead to a rough surface morphology[5]. So it is necessary to dope Zn at a proper concentration to explore new CIZS.

CIZS thin films can be prepared by all kinds of methods, for instance, magnetron sputtering[6], co-evaporation[7] and electro-deposition[8], *etc*. For one-step sputtering, the deposition temperature is an important parameter which affects the elemental composition of CIZS films during the process. To our knowledge, there are few researches on effect of deposition temperature in the growth of CIS and CIZS thin films by one-step sputtering method. Therefore, it is worth exploring preparation high quality CIZS thin films by using one-step sputtering process without post-annealing treatment.

1 Materials and methods

1.1 Materials preparation

With solid state reaction of Cu$_2$Se and In$_2$Se$_3$ powders at 1:1 mol ratio, CIS target was synthesized by ball-milled. CIZS target was obtained by mixing 0.2 mol ZnSe with 0.9 mol CIS powder. Both two targets were 5% Se in excess because of Se loss during the synthesis of targets and the deposition of thin films. CIS and CIZS were pre-

sintered at 500℃ in Ar atmosphere, followed by being hot-pressed sintered to pellets at 650℃.

The distance between target and substrate was fixed at 6.5 cm. The chamber was evacuated by turbo molecular pump to 2×10^{-4} Pa before deposition. The thin films were deposited on glass with a flow of Ar gas in 20 sccm and the working pressure was about 1.0 Pa. All the thin films were deposited with 80 W RF power at room temperature (RT) and 300℃ for 1 h. The obtained CIS and CIZS thin films were named as CIS-RT, CIZS-RT, CIS-300 and CIZS-300 corresponding to their deposited temperature, respectively.

1.2 Test procedure

Through a field emission scanning electron microscopy (FESEM: Philips XL30FEOPT) with an energy dispersive X-ray analyzer (EDX), the chemical composition and surface micrograph was obtained. The structure and phase of thin films were analyzed by XRD using Cu Kα radiation (Rigaku DMAX2500, Japan) from 10° to 70° at 40 kV and 20 mA. The optical properties of thin films were studied by Raman spectra with a micro-Raman spectrometer (Jobin Yvon LabRAM HR 800UR). The wavelength of 488 nm was used as the excitation source with a power of 20 mW. The normal-incident transmittance spectra were recorded using a double beam ultraviolet-infrared spectrophotometer (PerkinElmer Lambda 950), from 150 nm to 2500 nm (0.37− 6.13 eV) with a resolution of 2 nm. All measurements were performed at RT.

2 Results and discussion

2.1 Composition analysis

Figure 1 presents chemical composition of CIS and CIZS theoretical value and their corresponding experimental results. It can be seen that chemical composition of thin films almost deviates from the corresponding targets. Specifically, Cu content of all thin films is lower than that of corresponding targets, while In content of all thin films is higher than that of corresponding targets. It is caused by the different sputtering yield of Cu and In elements. According to the sputtering theory, $Y=0.024 \alpha S_n(E)/U_o$, where Y is the sputtering yield, α is a dimensionless constant, $S_n(E)$ is the nuclear stopping power and U_o is the surface binding energy per atom. In this equation, the surface binding energy U_o is inversely proportional to sputtering yield Y, so higher surface binding energy will lead to a lower sputtering yield. Since the surface binding energy of Cu (with 3.503 eV/atom) is higher than that of In (with 2.495 eV/atom), which may lead to the lower Cu content of films than that
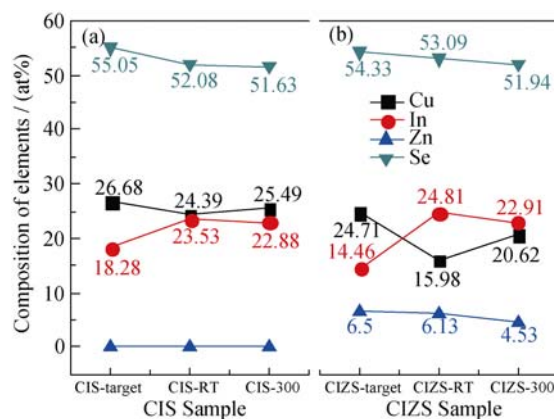

Fig. 1 Chemical composition of CIS, CIZS theoretical value and their corresponding experiment results

of targets during the sputtering process[4]. Furthermore, for CIZS-RT thin film, the Cu concentration is far deviated while the content of Zn is near stoichimetric ratio compared with the CIZS target. That is also due to the fact that Cu has the highest surfacing binding energy, while Zn has the lowest binding energy U_o (with 1.350 eV/atom) during sputtering process.

As shown in Fig. 1, Cu content of all thin films increases when substrate temperature increases up to 300℃. This increasing Cu percentage is attributed to the evaporation and decrease of In, Zn and Se. Furthermore, compared CIZS-RT with CIS-RT thin film, the concentration of In and Se in CIZS-RT thin film are enhanced while Cu concentration decreases. This phenomenon may be due to the antisite substitution among cations in CIZS thin films[5].

2.2 XRD Characterization

Figure 2 shows the XRD patterns of CIS and CIZS thin films and their related targets. As shown in Fig. 2, most samples have three strong peaks (112), (204/220) and
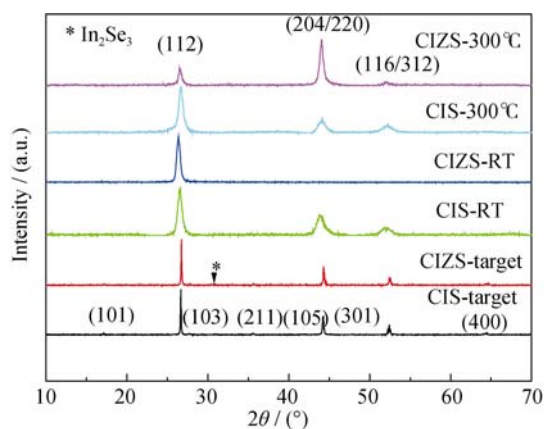

Fig. 2 Normalized XRD patterns of CIS target, CIZS target and their corresponding thin films deposited at room temperature and 300℃

(312/116), which are in accordance with JCPDS 65-4869. It can be seen that (112)-orientation is dominant for CIS-RT, CIS-300 and CIZS-RT samples, while grains of CIZS-300 thin film is the (220) preferred orientation. Higher deposited temperature and Cu-poor surface would induce the preferred orientation from (112) to (220) according to the studies reported by Contreras and Zhou, *et al*[9-10]. In our previous work, the relationship between preferred orientation of grains and substrate temperature with Cu-poor surface has been verified through varying the substrate temperature from RT to 400℃ in Ref. [10]. In this experiment, CIS-300 and CIZS-300 thin films deposited at the same temperature, however, CIS-300 is of Cu-rich state (*i.e.* Cu/In>1) and CIZS-300 is of Cu-poor state (Cu/(In+ Zn)<1). Cu-rich thin films under the similar growth conditions tend to be randomly oriented, and the possibly existed Cu-Se phase during growth of Cu-rich thin film may hinder the attainment of the (220) preferred orientation. CIZS-300 sample is grown at high deposited-temperature and it is Cu-poor. Therefore, grains of CIZS-300 thin film are the (220) preferred orientation which is different from other three samples.

2.3 Raman Spectra

Figure 3 shows the Raman spectra of CIS and CIZS thin films. It is obvious that there are two peaks around 171 and 206 cm^{-1}, which are assigned to the characteristic peaks of CIS phase. The main peak at 171 cm^{-1} is assigned to the A$_1$ mode, which has a purely ionic nature and originates from vibrations of Se atom in <001> plane [11]. The weak peak around 206 cm^{-1} corresponds to the B$_2$ mode of CIS and CIZS thin films, which is an evidence for growing CIZS chalcopyrite structure. No impurity phase can be found implying that all thin films are single phase. The intensity and frequency in Raman spectra are strongly related to chemical composition and defect in thin films[12]. Compared CIS with CIZS thin films, it is seen that the peaks of CIZS thin films are general
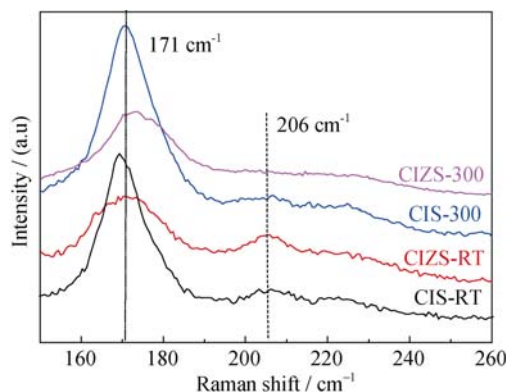
broadened and shift to a higher wave number. That might be due to Zn doping, which causes the decline of Cu concentration, and substitution of Zn for Cu in thin films. Moreover, compared CIS-RT with CIS-300 thin films, the main peak of CIS-RT is around 169 cm^{-1}, while the peak shifts to 171 cm^{-1} in CIS-300. The main peak shifts to high wave length, which is attributed to different composition deviation among the thin films[13].

2.4 Transmission Spectra

Figure 4 shows the transmission spectra of CIS and CIZS thin films. It can be seen that the transmittance of CIS thin films is much lower than that of CIZS thin films, which is due to the rough surface morphology. CIS thin films are rougher than CIZS thin films and CIS-300 is rougher than CIS-RT in the cross-sectional images. So the transmittance of CIS-RT is higher than that of CIS-300 and the transmittance of CIS thin films is much lower than CIZS thin films.

The optical band gap (E_{opt}) of the thin film is determined by extrapolating the straight line of ($\alpha h v$)^2 against to photon energy hv (eV) to the intercept on horizontal photo energy axis. In the Fig. 5, it can be seen that E_{opt} of CIZS-RT and CIZS-300 are 1.22 and 1.16 eV, while the E_{opt} of CIS-300 and CIS-RT are 0.98 and 1.04 eV, respectively. It is obvious that the E_{opt} of CIS thin films are smaller than that of CIZS thin films. The chemical composition plays an important role in the band gap of thin-films. When the Cu content decreases, the band gap of thin film increases because of a reduced Se p-Cu d interband repulsion. Based on the chemical composition in Table 1, the CIS thin films are of Cu-rich state, while CIZS thin films are Cu-poor state[14]. Therefore, the E_{opt} of CIS thin films is smaller than that of CIZS thin films. Moreover, the Cu content of thin films deposited at 300℃ is relatively higher than that of thin films deposited at RT. So the E_{opt} of thin films deposited at 300℃ is smaller than that of the thin films deposited at RT. Furthermore, for CIZS thin films, Zn acts as the donor and
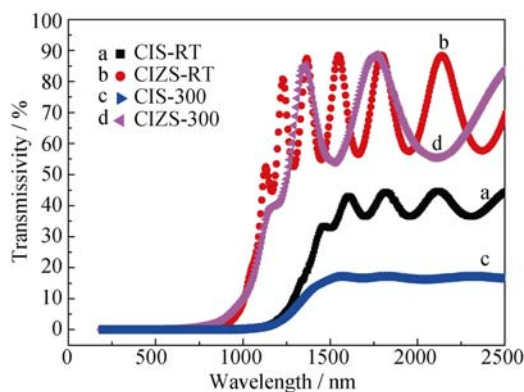

Fig. 3   Raman spectra of CIS and CIZS thin films deposited at with different substrate temperatures

Fig. 4   The transmittance of CIS and CIZS thin films deposited at RT and 300℃, respectively
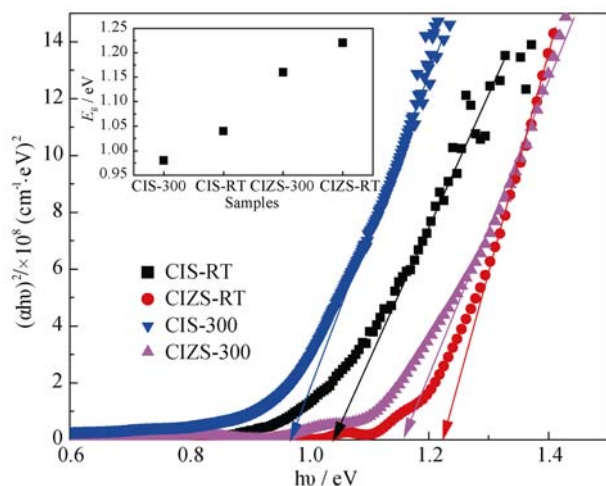
Fig. 5　E_{opt} of CIS and CIZS thin films deposited at RT and 300℃, respectively

acceptor in the CIS thin films and substitutes on the Cu and In lattice, respectively[15]. In the view of cation elec tron Eoptativity effect, the increasing optical band gap can be attributed to Zn altering the cation-anion bond length, which makes the E_{opt} ranging from 1.0 eV to 1.25 eV[16].

2.5　Surface morphology

Figure 6 shows the SEM surface micrographs and cross-sectional images of CIS and CIZS thin films. As shown in Fig. 6(a), the CIS-RT film surface is slightly rough and there some large conglomerates scattered over the sur-

face. This nonuniform surface possibly results from the large surface mobility during thin film growth. It is obvious that CIS-300 thin film surface shown in Fig. 6(c) is well-organized and the large scattered conglomerates disappear with the temperature increase. The surface morphology of the CIZS thin films showed in Fig. 6(b) and (d) is smoother, denser and more compact than that of CIS thin film. It may be due to the role of Zn as an additional nucleation site, which increases the number of grain boundaries and decreases the grain sizes of CIZS thin films[5].

3　Conclusions

CuInSe₂ and Cu₀.₉In₀.₉Zn₀.₂Se₂ thin films were deposited on glass substrates directly from CIS and CIZS targets by one-step RF magnetron sputtering process. The effect of Zn doping and substrate temperature on structure and optical properties of thin films was investigated. EDX and XRD results demonstrate that the preferred orientation of grains changes from (112) to (220), which can be attributed to appropriate substrate temperature and the variety of Cu content. Raman Spectra show a strong peak around 171 cm⁻¹ and a weak peak around 206 cm⁻¹, and the peaks shift and broaden with the Zn doping. From the transmission spectra, E_{opt} of CIZS thin films are larger than that of CIS thin films due to the variety of chemical composition. According to SEM, Zn doping can improve the surface morphology of thin films.
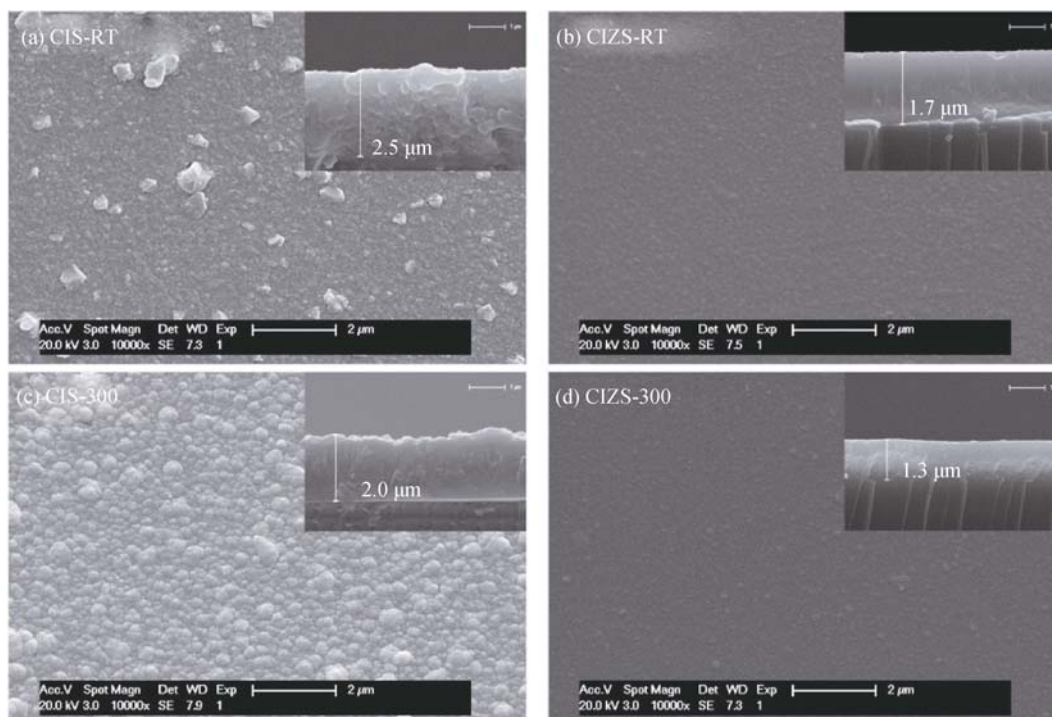

Fig. 6　SEM surface micrographs and cross-sectional image of CIS and CIZS thin films

References:

[1] ZARETSKAVA E P, GREMENOK V F. Correlation between Raman spectra and structural properties of $Zn_{2-2x}Cu_xIn_xSe_2$ films. *Optics and Spectroscopy*, 2007, **102(1):** 77–82.

[2] GREMENOK V F, ZARETSKAVA E P, SIARHEVEA V M, *et al*. Investigation of $CuInZnSe_2$ thin films for solar cell applications. *Thin Solid Films*, 2005, **487(1/2):** 193–198.

[3] SCHORR S, TOVAR M, SHEPTVAKOY D, *et al*. Crystal structure and cation distribution in the solid solution series 2(ZnX)–$CuInX_2$ (X=S, Se, Te). *Journal of Physics and Chemistry of Solids*, 2005, **66:** 1961–1965.

[4] SUN L, HE J, CHEN Y, *et al*. Comparative study on Cu_2ZnSnS_4 thin films deposited by sputtering and pulsed laser deposition from a single quaternary sulfide target. *Journal of Crystal Growth*, 2012, **361:** 147–151.

[5] WIBOWO R A, KIM K H. Band gap engineering of RF-sputtered $CuInZnSe_2$ thin films for indium-reduced thin-film solar cell application, *Solar Energy Materials and Solar Cells*, 2009, **93:** 941–944.

[6] HE J, SUN L, Ding N F, *et al*. Single-step preparation and characterization of $Cu_2ZnSn(S_xSe_{1-x})_4$ thin films deposited by pulsed laser deposition method. *Journal of Alloys and Compounds*, 2012, **529:** 34–37.

[7] VARELA M, BERTRAN E, MANCHON M, *et al*. Optical properties of co-evaporated $CuInSe_2$ thin films. *Journal of Physics D: Applied Physics*, 1986, **19:** 127–136.

[8] NAKAMURA S, SUGAWARA S, HASHIMOTO A, *et al*. Composition control of electrodeposited Cu-In-Se layers for thin film $CuInSe_2$ preparation. *Solar Energy Materials and Solar Cells*, 1998, **50:** 25–30.

[9] FANG J F, PENG D C, Chen J W. Mechanism of forming (220/204)-oriented $CuInSe_2$ film on Al:ZnO substrate using a two-step selenization process. *Journal of Crystal Growth*, 2011, **321:** 106–112.

[10] WANG W J, HE J, ZHANG K Z, *et al*. Characterization of $Cu_{0.9}In_{0.9}Zn_{0.2}Se_2$ Thin Films Prepared by One-step RF Magnetron Sputtering Process, Proceeding of 2013 International Conference on Material Science and Environmental Engineering, 2013.

[11] ZARETSKAVA E P, GREMENOK V F, SCHMITZ W, *et al*. Raman spectroscopy of $(CuInSe_2)_{x-2}(ZnSe)_{1-x}$ thin films. *Phys. Status Solidi* (c), 2004, **11:** 3106–3109.

[12] SATOSHI Y, MAKOTO K, KIYOSHI T. Characterization of copper indium diselenide thin films by Raman scattering spectroscopy for solar cell application. *Japanese Journal of Applied Physics*, 1989, **28:** L1337–L1340.

[13] TSENG Y H, Yang C S, WU C H, *et al*. Growth mechanism of $CuZnInSe_2$ thin films grown by molecular beam epitaxy. *Journal of Crystal Growth*, 2013, **378:** 158–161.

[14] ZHANG S B, WEI S H, ZUNGER A. Defect physics of the CIS chalcopyrite semiconductor. *Physical Review B*, 1998, **57:** 9642–9656.

[15] BASKET J, STOLWIJK N A, WUERZ R, *et al*. Zinc diffusion in polycrystalline Cu(In, Ga)Se_2 and single-crystal $CuInSe_2$ layers. *Applied Physics Letters*, 2012, **101(7):** 074105-1-3.

[16] JAFFE J E, ZUNGER A. Theory of the band-gap anomaly in ABC_2 chalcopyrite semiconductors. *Physical Review B*, 1984, **29:** 1882–1906.

单靶磁控溅射制备铜铟硒和铜铟锌硒薄膜及其结构、光学性质研究

王伟君，何　俊，张克智，陶加华，孙　琳，陈　晔，杨平雄，褚君浩

(华东师范大学 电子工程系，极化材料与器件教育部重点实验室，上海 200241)

摘　要: 采用单靶磁控溅射法制备了铜铟硒(CIS)和铜铟锌硒(CIZS)薄膜。XRD 表征发现 CIZS-300 出现了与其它薄膜不同的择优取向，分析认为贫铜的状态和适宜温度可能促使薄膜择优取向从(112)向(220)转化；拉曼光谱在 171 cm^{-1} 处出现的较强峰，和 206 cm^{-1} 处出现的较弱峰，分别为 A_1 和 B_2 振动模式，而 Zn 的掺入导致 A_1 拉曼峰的宽化和蓝移；Zn 的掺入使 Cu 含量改变进而使 CIZS 禁带宽度增大，这是由于 Se 的 p 轨道和 Cu 的 d 轨道杂化引起的；SEM 测试结果表明 CIZS 薄膜表面比 CIS 表面更为紧密、平滑。

关　键　词: 磁控溅射；铜铟锌硒；锌掺杂

中图分类号: TQ174　　　　**文献标识码:** A